Stress and the Acicular Ferrite Transformation

S. S. Babu and H. K. D. H. Bhadeshia
Materials Science and Engineering A156 (1992) 1-9

8.1 Introduction

In spite of the microstructural differences, there is considerable evidence that acicular ferrite and bainite have similar transformation mechanisms. The microstructures differ only because of their nucleation site. Some of the similarities between bainite and acicular ferrite were summarised in section 1.2.6. In addition, results of previous chapters indicated following;

1. Both reactions stop when the austenite carbon concentration reaches a value where it becomes thermodynamically impossible to achieve diffusionless growth (chapter 4).
2. Acicular ferrite only forms below the bainite–start temperature.
3. The elimination of austenite grain surfaces by covering them with inert allotriomorphic ferrite leads to a transition from a bainitic to an acicular ferritic microstructure (chapters 4 & 5).

Transformation to both acicular ferrite and bainite causes displacements which are characterised as invariant–plane strains with large shear components (Fig. 8.1). Consequently, the growth of a plate of acicular ferrite or bainite is confined to a single austenite grain (*i.e.*, it is hindered by a grain boundary) since the coordinated movement of atoms implied by the shape change cannot, in general, be sustained across a border between grains in different crystallographic orientations. A further implication is that plates of acicular ferrite, like bainite, *always* have an orientation relationship with the parent phase which is within the Bain region. This is not necessarily the case when the transformation occurs by a reconstructive mechanism.

It is this last characteristic, the invariant–plane strain shape deformation, which forms the basis of the present investigation. Such a transformation is displacive, and can be regarded as a deformation mode which in addition to accomplishing a shape change, also alters the nature of the lattice. During transformation induced by a decrease in temperature, it is the chemical driving force which causes the deformation. However, the application of an appropriate external stress can provide a mechanical driving force which stimulates transformation without the need to undercool. Such effects are well established for bainite, where a tensile stress favours the development of crystallographic variants whose shape deformations comply most with the applied stress.

The purpose of this investigation is to verify the existence of a similar effect for acicular ferrite. As will be seen later, the specific kind of stress response investigated provides good evidence for the displacive mechanism of the transformation. Acicular ferrite is a prominent

phase in steel weld metals (primarily because they contain nucleating inclusions). There is a possibility that the residual stresses associated with welding may influence the development of the acicular ferrite microstructure.

The only previous study on the relationship between stress and acicular ferrite in mixed microstructures, is by Dallam and Olson (1989). The stress was mostly generated by cooling constrained samples, the transformation being followed by monitoring the sample diameter. Dallam and Olson concluded that there is little influence on the volume fraction of acicular ferrite.

As discussed later, a much more sensitive method of following stress-affected displacive transformation is to monitor the transformation strains along more than one direction (Bhadeshia *et al.*, 1991).

8.2 EXPERIMENTAL METHOD

Alloy 77 is chosen for this study. The welding conditions and the final deposit chemistry are listed in Table 2.1 and Table 2.2. The weld metal, in the as deposited conditions transforms to a bainitic microstructure, in spite of the presence of numerous inclusions of the kind necessary to nucleate acicular ferrite. This is because, in the absence of any allotriomorphic ferrite at the austenite grain boundaries, the boundaries are free to nucleate bainite which forms at an overwhelming rate and succeeds in stifling the intragranular formation of acicular ferrite. By reheating the weld metal and then partially transforming the austenite at an intermediate temperature (T_1) to form a thin, uniform layer of allotriomorphic ferrite at the austenite grain surfaces grain boundary nucleation of bainite can be stifled. Thereby the remainder of the austenite transforms to intragranularly nucleated bainite as the alloy is held at a temperature (T_2) below the bainite-start (B_S) temperature (chapter 4).

This two-stage heat treatment (Fig. 8.2) provides a convenient way of generating an acicular ferrite microstructure in a controlled manner. The calculated transformation temperatures in chapter 5 are taken as an aid to the design of the heat treatment (Table 8.1). The calculation methods have been discussed before.

The heat treatment can easily be carried out in the *Formaster* thermomechanical simulator used in the present studies. The machine is equipped to simultaneously monitor and record the diameteral ($\frac{\Delta R}{R}$) and longitudinal strains ($\frac{\Delta L}{L}$), in addition to time, temperature and load data. It can be programmed to automatically carry out the specified thermomechanical treatments. The samples were in the form of 8 mm diameter cylinders 12 mm in length, made from the weld metal by rolling, swaging and machining (Fig. 2.4). The specimen preparation has been presented in chapter 2. The simulator experiments were carried out with the specimen chamber filled with argon. The rapid temperature changes needed between T_1 and T_2, and between T_2

Table 8.1 Calculated transformation data for alloy 77.

Ae_3	828 °C
W_S	680 °C
B_S	546 °C
M_S	427 °C

and ambient temperature were achieved using argon gas jets. Since the equipment is fully capable of monitoring the transformation during these rapid changes, it was confirmed that no reaction occurred during the gas quenching process, so that all the transformation could be attributed to isothermal reaction at T_1 and T_2. The thermomechanically treated samples were examined in both their transverse and longitudinal sections using the usual metallographic techniques. The austenite grain sizes were determined to be 151 ± 23 μm, defined as the mean lineal intercept of random test lines superimposed on the microstructure.

8.2.1 The Applied Stress

The stress was only applied the instant the sample reached T_2, in order to influence the development of acicular ferrite. It was intended in this work to limit the applied stress to a value below the yield strength of austenite. Any plastic deformation can complicate interpretation because the resulting defect structure can either assist or interfere with the progress of transformation. Published data on the yield strength of austenite as a function of temperature (Fig. 8.3) were extrapolated to estimate its yield strength to be approximately 500 MPa over the temperature range 500–550 °C. Even if the extrapolation is unjustified, the yield strength cannot be less than about 200 MPa, which corresponds to experimental data from 750 °C (Fig. 8.3). Consequently, the experiments were carried out at two load levels, both of which should be well below the austenite yield strength at T_2: the chosen loads correspond to stress levels of 116 and 174 MPa. The results of these experiments should be compared against transformation without the influence of any applied stress. However, under the conditions of the experiments, the longitudinal strain cannot be recorded unless a small stress of about 12 MPa is applied, since the cross head uses this signal to follow the dimensional changes in that direction. Consequently, the "zero stress" experiments described here in fact were carried out with the 12 MPa stress during transformation. The details of the actual experiments are listed in Table 8.2; the calculated time–temperature–transformation diagram presented in Fig. 6.1 (for alloy 77) confirms that the transformation temperatures are chosen to first cause the growth of allotriomorphic ferrite and then of acicular ferrite.

Table 8.2 Heat Treatment Schedule of the experiments. In each case the austenitisation heat treatment was carried out at 1150 °C for 10 minutes. The stress was applied immediately after the sample reached T_2. t_1 and t_2 are the time periods spent by the sample at the temperatures T_1 and T_2 respectively. The prefix "ST" on the specimen identification indicates transformation under the influence of a large stress which is nevertheless below the yield strength of the austenite and "NST" corresponds to the no stress experiment (see text).

Identification	T_1 °C/ t_1 s	T_2°C/ t_2 s	Stress MPa
NST0	660 / 120	530 / 300	12
NST1	660 / 120	500 / 300	12
NST2	660 / 120	500 / 300	12
ST1	660 / 60	530 / 300	116
ST2	660 / 120	530 / 300	116
ST3	660 / 120	530 / 300	174
ST4	660 / 120	500 / 300	116

8.3 Results and Discussion

8.3.1 The Microstructure

Throughout these experiments, it was our aim to demonstrate a clear effect of stress. The clarity of microstructural changes can be maximised by only partially transforming the austenite to acicular ferrite, and allowing the remainder to decompose by a martensitic transformation during the quench to ambient temperature. Two transformation temperatures were therefore studied, both quite close to the calculated B_S temperature (546 °C). This ensures that the amount of acicular ferrite that forms is limited, because that amount increases from zero at B_S to a quantity determined by the T_0' curve of the phase diagram as the temperature is reduced below B_S.

Specimens NST0 and NST1 which are from the zero stress experiments showed similar microstructures, NST1 having a larger quantity of acicular ferrite, as expected from its lower T_2 transformation temperature. The microstructure of NST1 is illustrated in Fig. 8.4a. It reveals the thin continuous layer of allotriomorphic ferrite which grew and covered the austenite grain boundaries at T_1; in addition, there is the intragranularly nucleated acicular ferrite which formed at T_2. The acicular ferrite microstructure is as expected in normal welds, with plates pointing along many directions. Sample NST2 represents a repeat of the treatment given to

NST1. It was used for confirmation of the experimental method during the initial work when the experimental scheme was being designed. Its microstructure was found to be identical to that of NST1.

Fig. 8.4b–e are longitudinal sections of samples ST1–4; the direction of the applied stress is indicated on each of the micrographs. All of these experiments reveal a dramatic change in the microstructure when the acicular ferrite forms under the influence of the applied stress. The number of crystallographic variants per grain is reduced drastically and there is a strong tendency for the plates that do grow to align within any given prior austenite grain.

These results are easily understood once it is accepted that acicular ferrite growth leads to an invariant–plane strain (IPS) change in the transformed region (Strangwood and Bhadeshia, 1987a). A uniaxial compressive stress will oppose the dilatational component of this IPS (Patel and Cohen, 1953), but the shear component will interact favourably. Since the shear component is much larger than the dilatational strain, the overall interaction of the shape change with the strain can be favourable. The compressive stress resolves to give maximum shear stresses on planes which lie at 45 ° to the stress axis. Given that the samples used are polycrystalline, it is only by fortuitous circumstance that the crystallographic orientation of a particular austenite grain permits acicular ferrite to form on these planes of maximum shear stress. Nevertheless, acicular ferrite variants which happen to be most parallel to those planes are expected to be favoured by the stress, and will form preferentially. This is what leads to the development of the aligned microstructure illustrated in Fig. 8.4b–e. It is noteworthy that there are in principle up to 24 different crystallographic variants of acicular ferrite possible within each austenite grain. Of these, it is likely that one or more may lie fairly close to the 45 ° orientation. Indeed, it is easy to see from Fig. 8.4b–e that the acicular ferrite plates that grow tend to lie fairly close to the optimum orientation.†

One further observation is relevant; Fig. 8.5 shows higher magnification images of samples NST1 and ST2. It is evident that acicular ferrite tends not to form in the regions of austenite adjacent to the allotriomorphs of ferrite. This is exactly as predicted by theory, that the partitioning of carbon during the growth of the allotriomorphs enriches the adjacent austenite which consequently becomes more stable to transformation when compared with unaffected austenite.

8.3.2 The Transformation Strains

Given the nature of the invariant–plane strain shape change (Fig. 8.1), the transformation strain can only be isotropic if the effects of many different randomly orientation crystallographic

† In fact, although the plane of maximum shear stress is at 45 degrees to the stress axis, the most favoured plane is calculated by also taking into account the dilatational component of the IPS. However, since that component is rather small, 45 degrees is a good approximation for the optimum orientation.

variants are averaged. The shear components would then tend to cancel out, and the dilatational component of the shape change would appear to be like a uniform volume expansion instead of a uniaxial strain normal to the habit plane. This kind of behaviour might be expected in a random, fine grained polycrystalline sample of austenite.

However, if the sample is crystallographically textured, or if the variants do not form at random, then the transformation strain cannot be isotropic, and the net strain along any particular direction may contain contributions from both the shear and dilatational terms. It then becomes possible to detect transformation plasticity as well as volume change.

The strain measurements are presented in Fig. 8.6. In the absence of stress or crystallographic texture, both the longitudinal and radial strains are expected to be positive since only the volume change is detected. As is seen from 8.6, this is true during the initial stages of transformation (NST1, NST2), but not in the later stages, probably because of the small stress of 12 MPa used for these samples, but possibly also because of crystallographic texture in the samples.

For all other samples (ST1–4), the longitudinal strain is always negative as the specimen transforms in a manner which tends to accommodate the applied compressive stress, whereas the radial strains are all positive. The experiments provide impressive proof of the shape deformation accompanying the displacive growth of acicular ferrite. It would be impossible to explain both the magnitude and signs of the strains detected on the basis of a reconstructive transformation mechanism.

More detailed interpretations of these data require methods of accurately deconvoluting the measured strains into the volume change and transformation plasticity terms. That problem is currently under investigation.

8.4 Conclusions

It is found that the acicular ferrite microstructure responds to stresses below the yield strength of the austenite. The response is in fact quite remarkable, the stress favouring the development of specific crystallographic variants. This leads to a destruction of the conventional acicular ferrite structure in which the plates emanating from inclusions point in many different directions. Apart from these microstructural changes, the measured strains during transformation under the influence of stress give conclusive proof for the shape deformation and displacive mechanism of acicular ferrite growth.

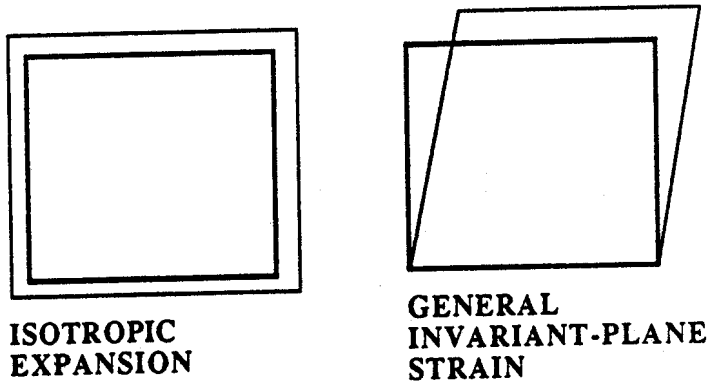

Fig. 8.1 Schematic explanation of shape changes due to isotropic volume change and a general invariant plane strain. The invariant plane strain in austenite to displacive ferrite products involve shear and a dilatational component (Bhadeshia *et al.*, 1991).

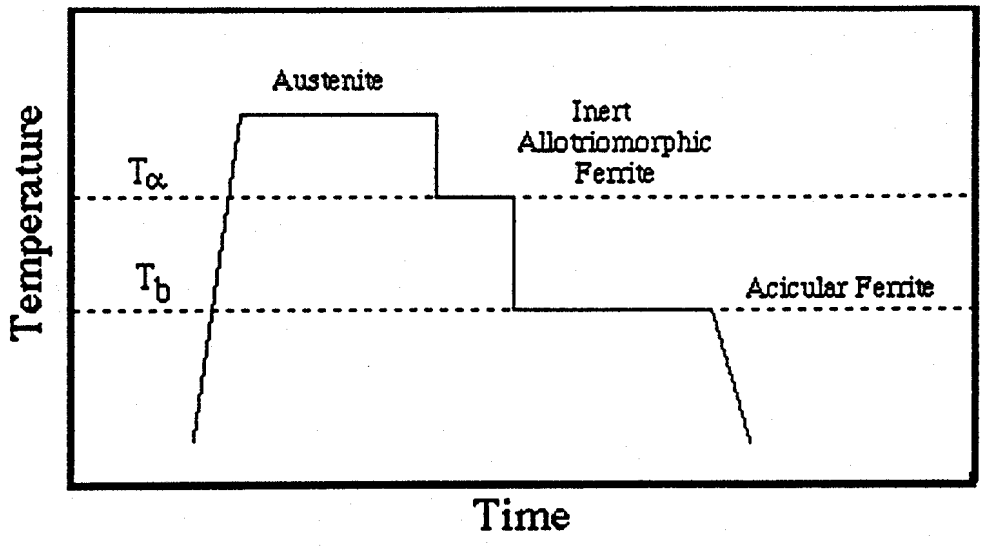

Fig. 8.2 Schematic illustration of two stage heat treatment schedule for generating acicular ferrite microstructure.

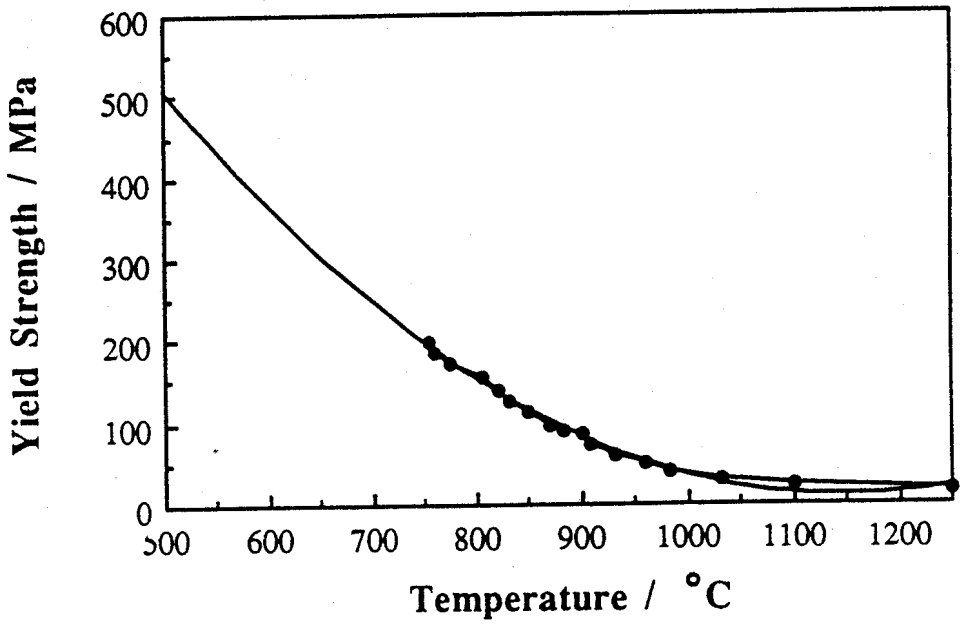

Fig. 8.3 Variation of yield strength as a function of temperature. The graph also contains two extrapolation curves in estimating the yield strength of austenite at around 500 - 550 °C. The experimental data points are for a Nb-V microalloyed steel (Weiss *et al.*, 1981).

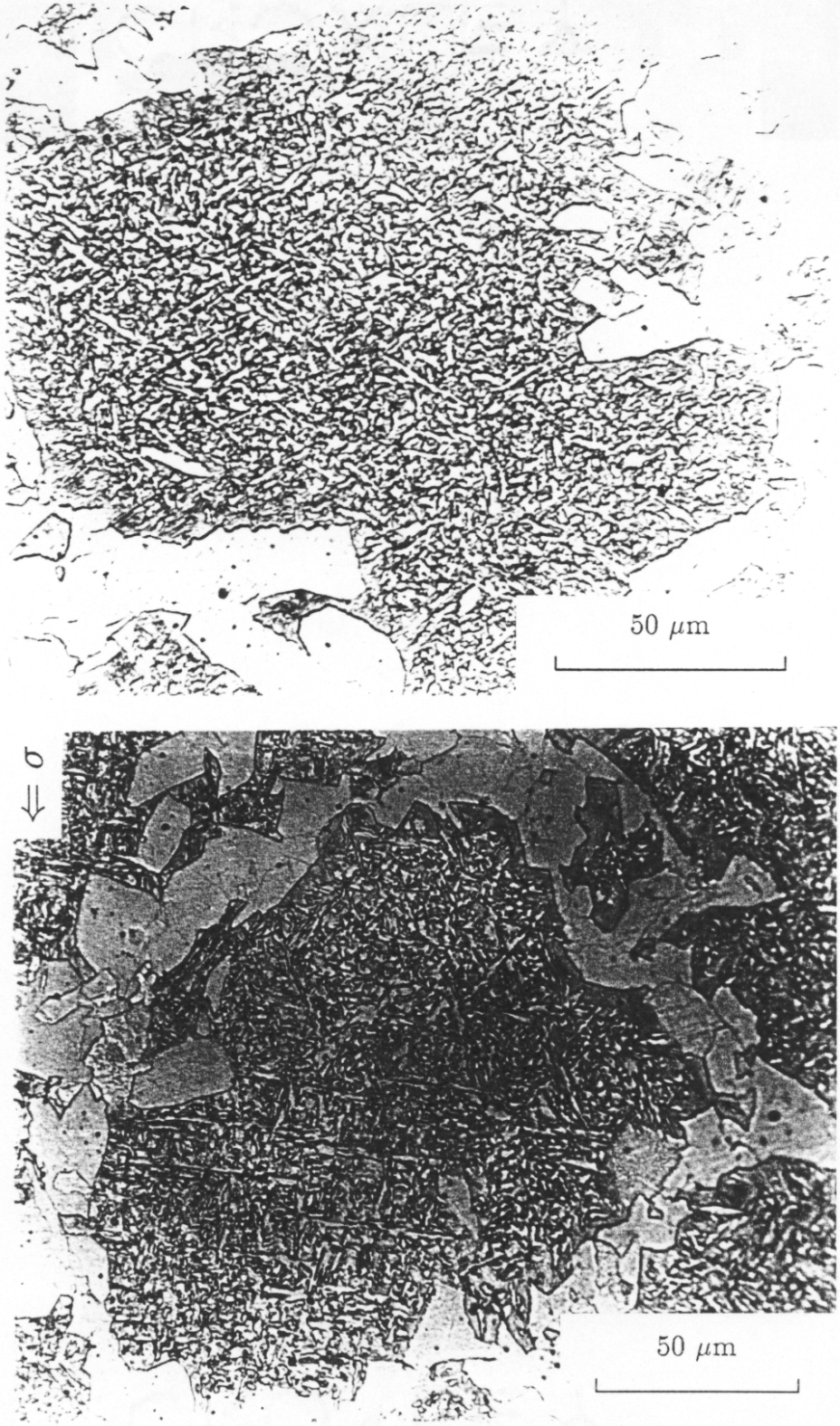

Fig. 8.4 Microstructure observed in no stress experiments and stressed samples. For each case there are two microstructures corresponding to the transverse and longitudinal directions. The arrows in the longitudinal section micrographs indicate the stress direction. The details and the heat treatments are given in the Table 8.2; (a) NST1,

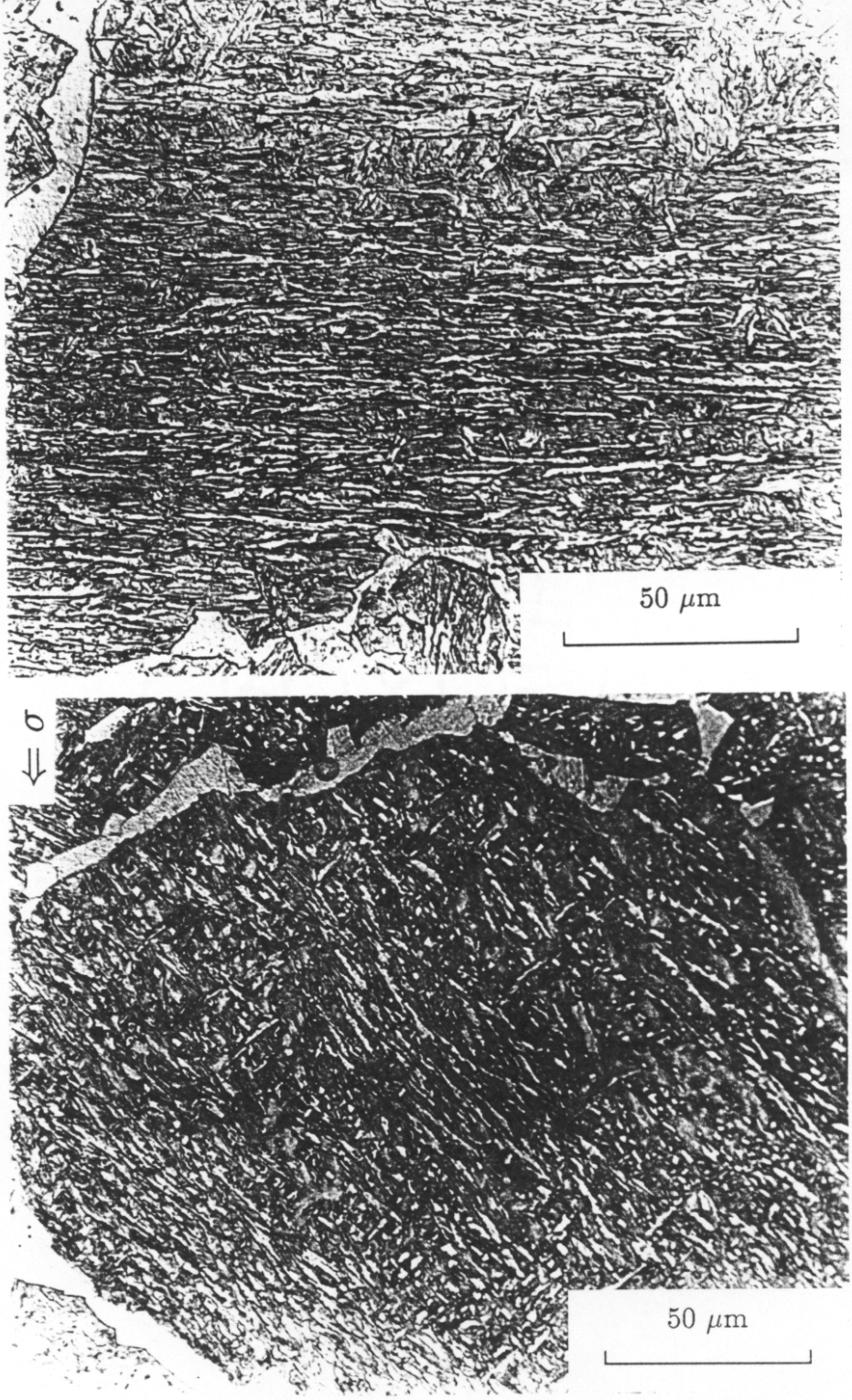

Fig. 8.4 continued...

(b) ST1,

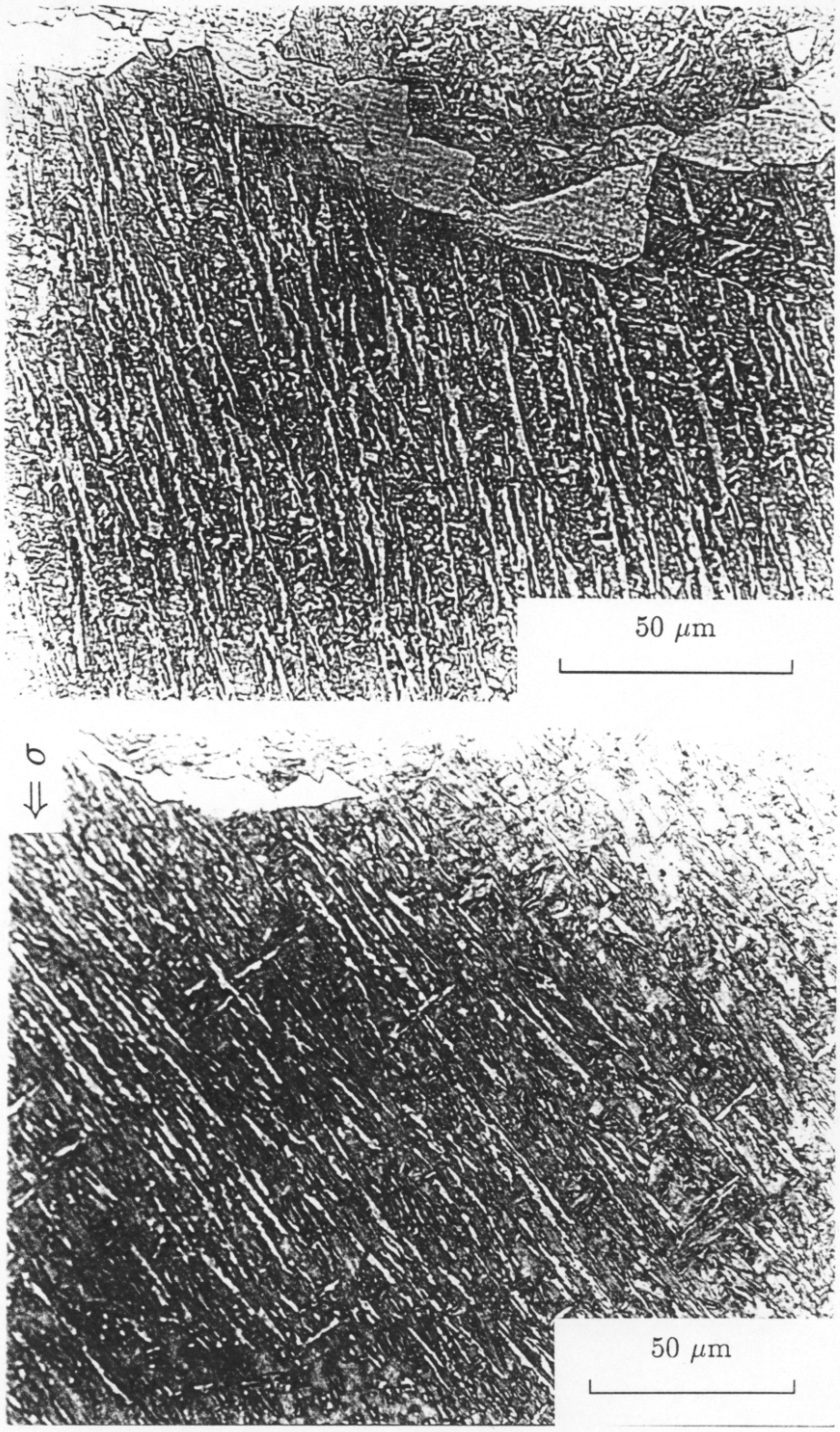

Fig. 8.4 continued...

(c) ST2,

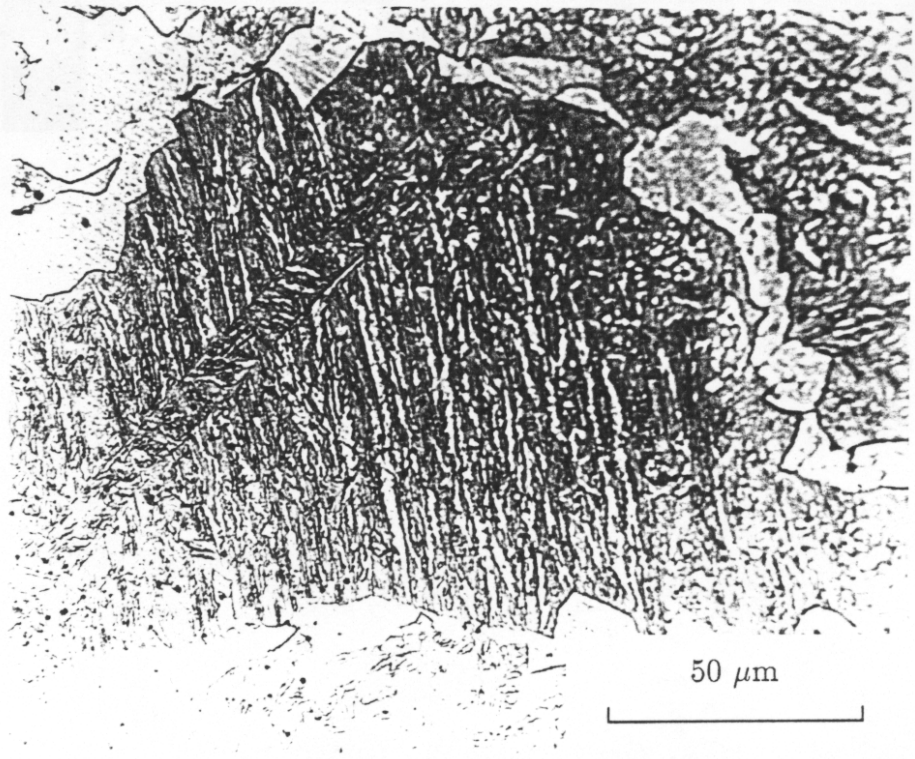

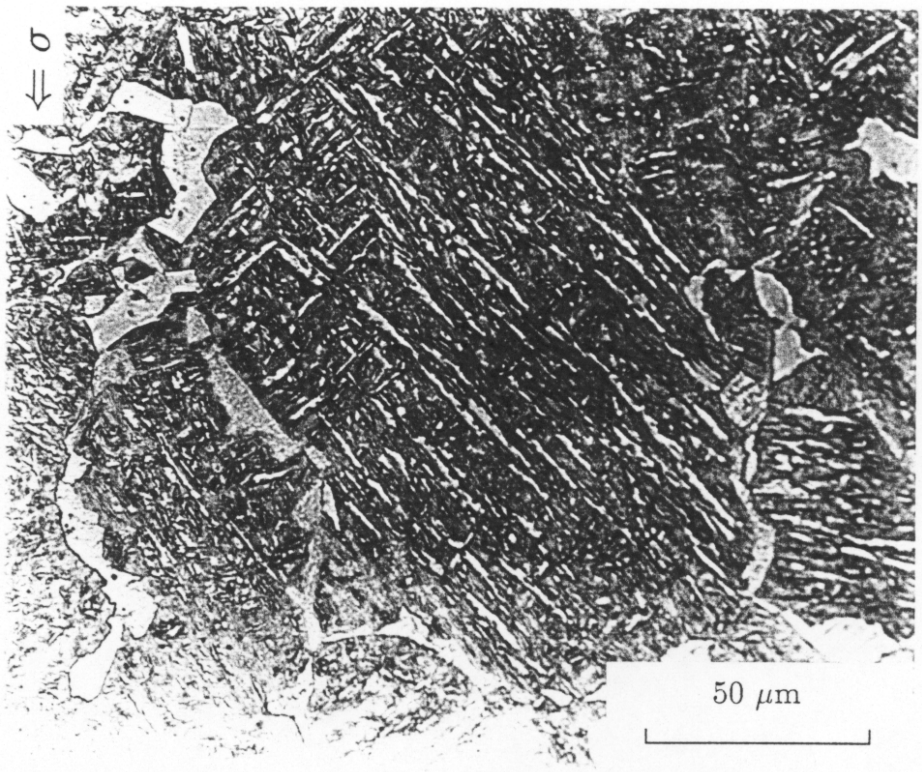

Fig. 8.4 continued...

(d) ST3,

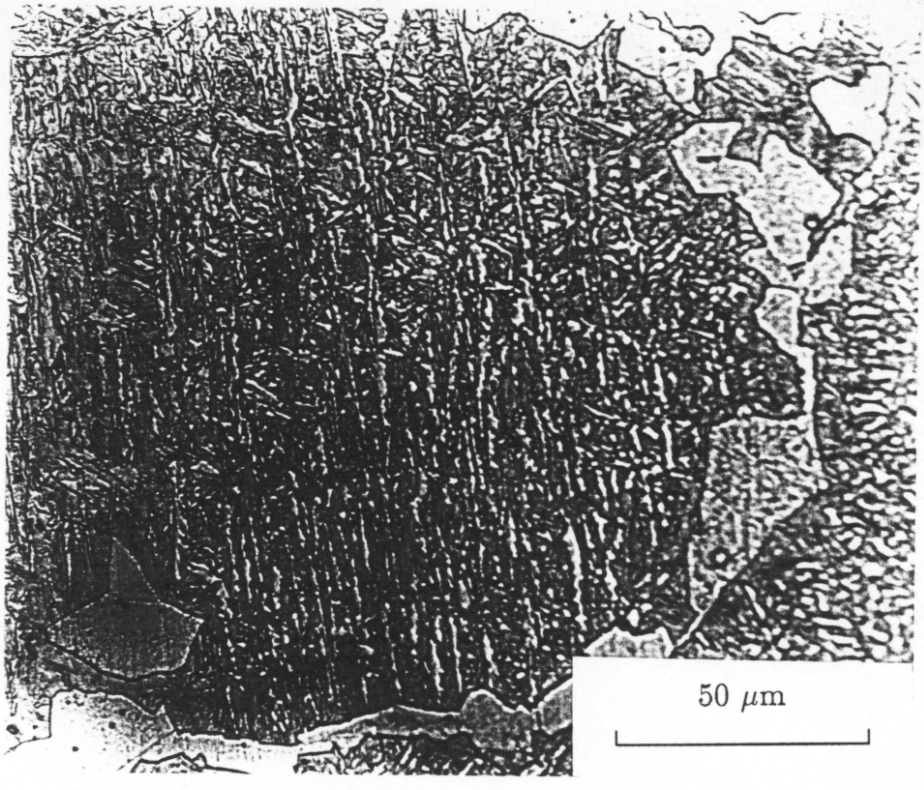

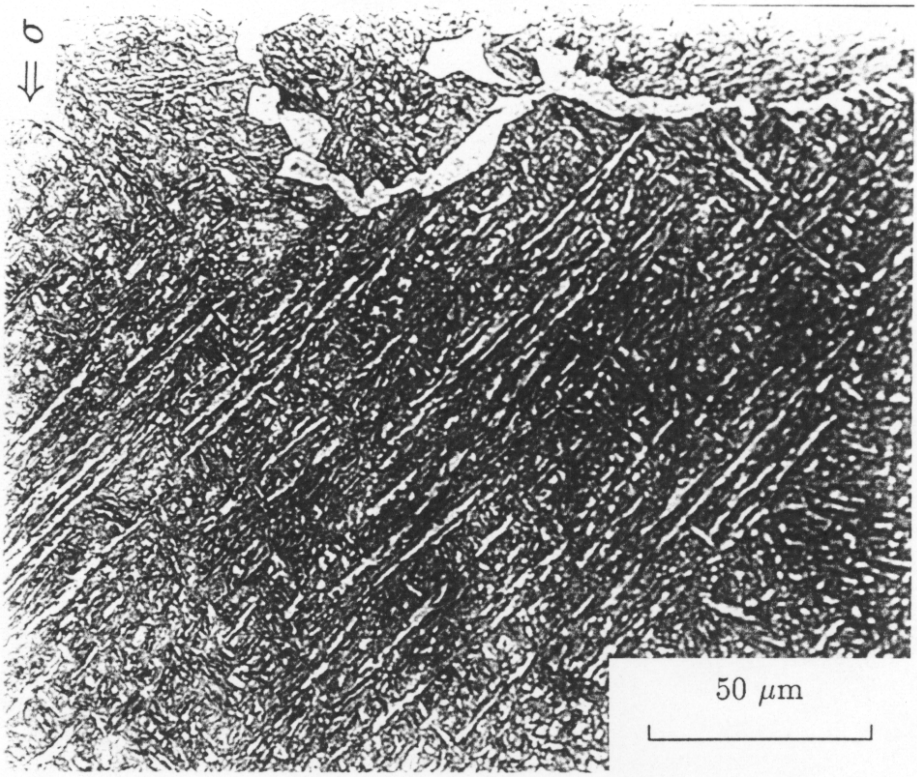

Fig. 8.4 continued...

(e) ST4

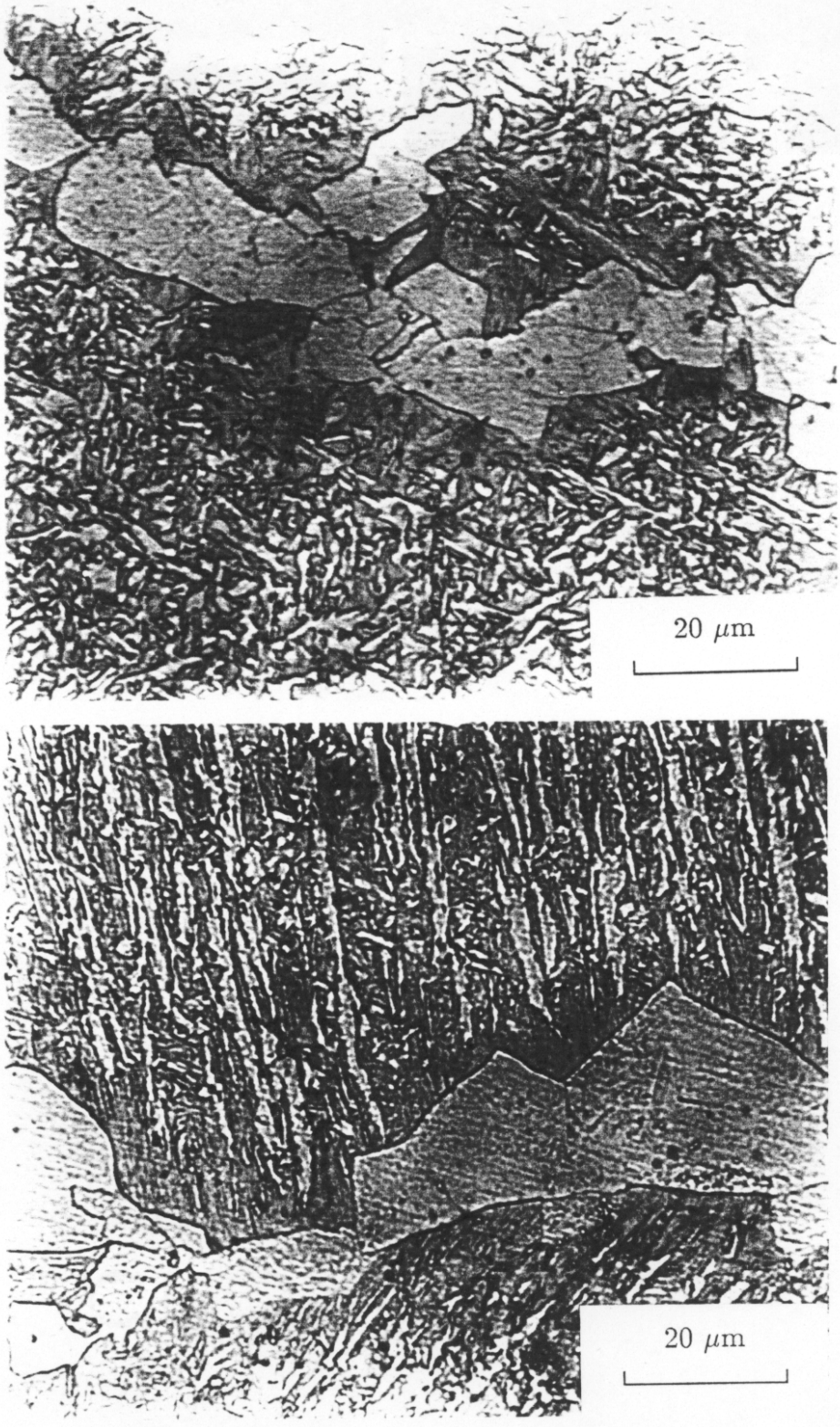

Fig. 8.5 Microstructure of (a) NST1 and (b) ST2 at higher magnification. The micrograph illustrates the transformation free zone around the allotriomorphic ferrite interface.

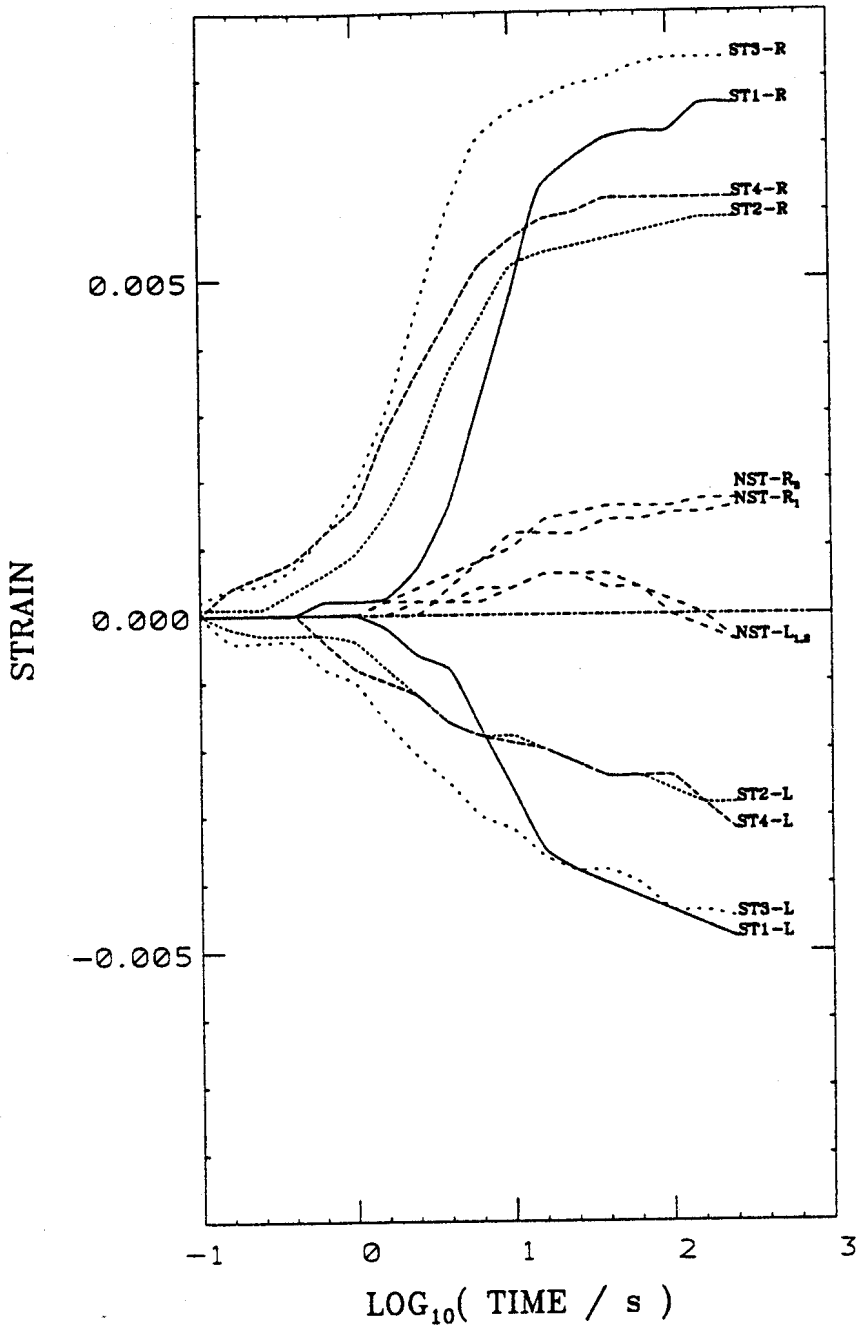

Fig. 8.6 Plot of transformation strain in the longitudinal and transverse directions as a function of time for all the experiments listed in Table 8.4. Here the letter 'R' represents the diametaral strain $\frac{\Delta R}{R}$ and 'L' represents longitudinal strain $\frac{\Delta L}{L}$.